



Treatment With FoxP3+ Antigen-Experienced T Regulatory Cells Arrests Progressive Retinal Damage in a Spontaneous Model of Uveitis

OPEN ACCESS

Edited by:

Michele Marie Kosiewicz,
University of Louisville, United States

Reviewed by:

Hui Shao,
University of Louisville, United States

Darren James Lee,
The University of Oklahoma Health
Sciences Center, United States

*Correspondence:

John V. Forrester
j.forrester@abdn.ac.uk

† These authors have contributed
equally to this work and share first
authorship

* Present address:

Yi-Hsia Liu,
Wolfson Wohl Cancer Research
Centre, Institute of Cancer Sciences,
University of Glasgow, Bearsden,
United Kingdom

Kimmo Makinen,
Human Health, Novozymes A/S,
Bagsvaerd, Denmark
Koji Kamoi,
Department of Ophthalmology and
Visual Science, Graduate School of
Medical and Dental Science, Tokyo
Medical and Dental University, Tokyo,
Japan

Clare L. C. Corbett,
School of Life Sciences, University of
Nottingham, Nottingham,
United Kingdom
Izabela P. Klaska,
Institute of Ophthalmology, University
College London, London,
United Kingdom

Specialty section:

This article was submitted to
Autoimmune and Autoinflammatory
Disorders,
a section of the journal
Frontiers in Immunology

Received: 14 February 2020

Accepted: 29 July 2020

Published: 04 September 2020

Yi-Hsia Liu^{1†}, Christine Mölzer^{1†}, Kimmo Makinen^{1†}, Koji Kamoi^{1†}, Clare L. C. Corbett^{1†},
Izabela P. Klaska^{1†}, Delyth M. Reid¹, Heather M. Wilson¹, Lucia Kuffová¹,
Richard J. Cornall² and John V. Forrester^{1*}

¹ Institute of Medical Sciences, University of Aberdeen, Aberdeen, United Kingdom, ² MRC Human Immunology Unit, MRC Weatherall Institute of Molecular Medicine, University of Oxford, Oxford, United Kingdom

We specify the clinical features of a spontaneous experimental autoimmune uveitis (EAU) model, in which foreign hen-egg lysozyme (HEL) is expressed in the retina, controlled by the promoter for interphotoreceptor retinol binding protein (IRBP). We previously reported 100% P21 (post-partum day) IRBP:HEL single transgenic (sTg) mice, when crossed to transgenic T cell receptor mice (3A9) generating the double transgenic (dTg) genotype, develop EAU despite profound lymphopenia (thymic HEL-specific T cell deletion). In this work, we characterized the immune component of this model and found conventional dTg CD4+ T cells were less anergic than those from 3A9 controls. Furthermore, prior *in vitro* HEL-activation of 3A9 anergic T cells (T_{an}) rendered them uveitogenic upon adoptive transfer (Tx) to sTg mice, while antigen-experienced (AgX, dTg), but not naïve (3A9) T cells halted disease in P21 dTg mice. Flow cytometric analysis of the AgX cells elucidated the underlying pathology: FoxP3+CD25^{hi}CD4+ T regulatory cells (T_{reg}) comprised ~18%, while FR4+CD73+FoxP3-CD25^{lo/-}CD4+ T_{an} comprised ~1.2% of total cells. Further T_{reg}-enrichment (~80%) of the AgX population indicated FoxP3+CD25^{hi}CD4+ T_{reg} played a key role in EAU-suppression while FoxP3-CD25^{lo/-}CD4+ T cells did not. Here we present the novel concept of dual immunological tolerance where spontaneous EAU is due to escape from anergy with consequent failure of T_{reg} induction and subsequent imbalance in the [T_{reg}:T_{effector}] cell ratio. The reduced numbers of T_{an}, normally sustaining T_{reg} to prevent autoimmunity, are the trigger for disease, while immune homeostasis can be restored by supplementation with AgX, but not naïve, antigen-specific T_{reg}.

Keywords: autoimmune uveitis, cell therapy, adoptive transfer, hen-egg lysozyme, T cell anergy, anti-uveitogenic

INTRODUCTION

The relative contribution of T cell anergy (T_{an}) vs. regulatory T cells (T_{reg}) in the context of autoimmunity has become blurred as a result of recent studies in evaluating the relationship between T_{reg} and T_{an} (1). This has particular relevance to the development of customized cell therapies for immune-mediated diseases, some of which are close to clinical translation.

Standardized protocols for preparing T regulatory cells (T_{reg}) and tolerogenic dendritic cells (tolDC) have been proposed (2, 3) and are aimed at facilitating progress toward Phase III clinical trials for autoimmune and immune-mediated diseases (4) but limited account is taken of the role of T_{an} in these protocols (4). Uveitis is an immune-mediated/autoimmune disease of considerable morbidity (4–6) in which the inciting agent is obscure (7). Current treatment options are limited to disease control by steroids and biologics. Experimental models of autoimmune uveoretinitis (EAU) have been helpful in exploring disease mechanisms (8). Traditionally, EAU is induced by subcutaneous inoculation of retina-specific antigens (9) in complete Freund's adjuvant (CFA). However, such conventional models may not be representative of “non-infectious” human uveitis, which develops in the absence of an obvious trigger, i.e., spontaneously (7).

Critically, experimental models of spontaneous uveitis, mostly in genetically manipulated mice represent an important attempt to mimic clinical disease more closely. In some models, single transgenic (sTg) mice express “foreign” antigens such as β -galactosidase or hen egg lysozyme (HEL) in the retina or lens under the control of a tissue-specific promoter such as rhodopsin, α -crystallin, arrestin, or interphotoreceptor retinol binding protein (IRBP). Uveitis can either be induced after adoptive transfer (Tx) of antigen-specific T cells (10) or develops spontaneously in F1 mice after crossing sTg mice to antigen-specific T cell receptor (TCR) mice, thus generating the double-transgenic (dTg) HEL/TCR genotype (11). In the IRBP:HEL sTg mouse model, HEL protein is photoreceptor membrane-bound, linked to the MHC class I protein. In dTg mice EAU develops with a 100% frequency (11), while 3A9 TCR (HEL-specific) mice do not develop uveitis. Both rhodopsin-HEL and IRBP:HEL sTg mice develop a degree of retinal photoreceptor shortening without inflammation, which, in the case of IRBP:HEL sTg mice is associated with reduced levels of IRBP. This retinal degeneration is age-related and has no impact on the development of EAU in dTg mice which has its onset at P21 when the retina is normal and there is abundant retinal HEL expression (12).

In the present study, we report that dTg mice undergoing extensive thymic clonal deletion of HEL-specific CD4⁺ T cells with profound lymphopenia evident from P20/21 (11), develop clinical signs of EAU at the same time with focal patches of retinal vasculitis and infiltration of the retina by Th1 and Th17 cells. Spontaneous development of EAU in dTg mice correlates with both, lymphopenia affecting particularly the T_{reg} compartment, and limited T cell anergy. Adoptive transfer of HEL-specific (1G12⁺) CD3⁺CD4⁺CD8⁻ conventional T cells (T_{conv}) to young (P21) sTg mice also causes EAU in a dose-dependent manner. Pathogenic T_{conv} cells secrete both IFN γ and IL17/IL22 and require activation by HEL *in vitro* to induce EAU on Tx. HEL-specific (1G12⁺) CD3⁺CD4⁺CD8⁻ double negative (DN) cells are also present in dTg mice but are not pathogenic.

Interestingly, Tx of unfractionated antigen-experienced (AgX, P60) lymph node T cells from dTg mice with end-stage EAU, but not lymph node (LN) cells from 3A9 TCR mice, arrested the development of EAU and even reversed disease. FoxP3⁺CD25⁺ T_{reg} were found to be the suppressive T cell

population. These data attest to an imbalance between T_{reg} and T_{eff} that permits spontaneously activated, poorly anergic T_{conv} to induce disease (13).

The mechanisms in pre-clinical models of EAU are under continued investigation. Here, we characterized in detail the immune component driving the pathogenesis of our spontaneous model of EAU. We furthermore show that (a) both limited anergy and an imbalance in [T_{reg}:T_{eff}] combine to permit development of spontaneous autoimmunity; that (b) treatment with AgX T_{reg} can prevent spontaneous autoimmunity; and that (c) protocols to generate T_{reg} *in vitro* may need to take into account the proportion of T_{an} in the cell preparation.

MATERIALS AND METHODS

Study Design

Transgenic IRBP:HEL mice were used to investigate in detail the clinical dynamics and severity of spontaneous autoimmune uveitis (EAU) in the dTg genotype, using *in vivo* and *in vitro* methodological approaches, including the therapeutic adoptive transfer of an enriched T_{reg} cell population.

Animals

The generation of dTg mice was previously described (11, 12). The procedures adopted conformed to the regulations of the Animal License Act (United Kingdom). All mice were bred in established breeding colonies and housed in a Medical Research Facility, University of Aberdeen. The genotype of the mice was verified by genotyping using standard in-house PCR procedures. Littermate male and female mice of different ages and genotypes were used in the experiments as specified, with 3A9 TCR mice serving as control animals.

Clinical Evaluation of Ocular Disease

Mice fundi were imaged using an otoscope-based fiber-optic light device as described previously (14). Following the Laboratory Animal Science Association's (LASA) good practice guidelines for administration of substances, mice were anaesthetized with an intraperitoneal injection of a mixture of 40 mg/kg Vetalar[®] (Fort Dodge Animal Health Ltd., Southampton, United Kingdom) and 0.2 mg/kg Domitor[®] (Orion Pharma, Espoo, Finland) diluted in injectable water. Pupils were dilated with Minims[®] 1% (w/v) Tropicamide, and 2.5% (w/v) Phenylephrine hydrochloride (both from Bausch & Lomb UK Ltd., Kingston-upon-Thames, United Kingdom). Viscotears[®] Carbomer 2 mg/g liquid gel (Alcon Eyecare UK Ltd., Camberley, United Kingdom) was applied to the corneal surface to protect the cornea from drying during imaging. Severity of disease was graded on the appearance and number of fundus lesions using an inflammation scoring system modified from Xu et al. (14) (**Supplementary Table 1**) and an atrophy scoring system (12) (**Supplementary Table 2**).

Histology

Mice (P16–60) were sacrificed and eyes removed immediately. One eye was fixed in 2.5% (w/v) glutaraldehyde (Fisher Chemicals, Loughborough, United Kingdom) and embedded

in resin for standard hematoxylin and eosin (H&E) staining. Images were collected using a ProgRes XT Core 5 color digital microscope camera (JENOPTIK Optical Systems GmbH, Jena, Germany) mounted on an inverted microscope (Carl Zeiss Axioskop 40, MicroImaging GmbH, Jena, Germany). The fellow eye was prepared for immunostaining.

Immunostaining

Freshly collected eyes were embedded in Tissue-Tek[®] OCT compound embedding medium (Sakura Finetek Europe B.V., Alphen aan den Rijn, Netherlands), and cryo-sections (7 μm) cut and fixed with cold acetone for 15 min at room temperature (20 ± 2°C). After 3 thorough washes, samples were blocked with 5% BSA for 30 min and were then incubated with the following antibodies (all purchased from BD Biosciences, Oxford, United Kingdom, unless stated otherwise): rabbit anti-HEL (Rockland Immunochemicals, Limerick, PA, United States; diluted 1:300 in PBS), anti-mouse CD4 FITC (GK1.5, 1:20), purified anti-mouse CD4 (clone GK1.5, 1:100), anti-mouse CD3 FITC (KT3, 1:20), anti-mouse MHCII FITC (28-16-8S, 1:20), biotinylated anti-mouse MHCII (28-16-8S, 1:20), anti-mouse CD11b FITC (M1/70, 1:100), purified anti-mouse CD11c (HL3, 1:50), purified anti-mouse CD8 (53-6.7, 1:100), anti-mouse F4/80 FITC (Cl:A3-1, 1:20) for 1h, followed by TRITC conjugated anti-rabbit IgG and Cy5-conjugated streptavidin (anti-HEL), Alexa 546-conjugated anti-rat streptavidin (for CD4), Alexa 546-conjugated anti-rat streptavidin (for MHCII), Alexa 546-conjugated anti-hamster streptavidin, Cy5-conjugated anti-hamster streptavidin (for CD11c), Alexa 546-conjugated anti-rat streptavidin (for CD8) for a further hour. The dilution factor of the secondary antibodies was 1:200. After staining, samples were washed and mounted with Hydromount[™] Aqueous Non-fluorescing Mounting Media (National diagnostics, Hull, United Kingdom), and photos taken using a Zeiss LSM510 confocal microscope (Carl Zeiss Meditec, Göttingen, Germany).

Flow Cytometry

Single cell suspensions of cells isolated from retinas and lymph nodes (15) were analyzed using flow cytometry. Both eye-draining (submandibular) and non-draining LN (superficial cervical and inguinal) were included. For analysis of eye-infiltrating cells, both retinal tissues were separated from the choroid. Retinas were digested for 40 min at 37°C in 1 ml PBS containing final conc. of 10 μg/ml Liberase and 10 μg/ml DNase I (both from Roche, Mannheim, Germany). Dissociated cells were washed and re-suspended in PBS containing 2% FBS for staining. Primary antibodies used (all from BD Biosciences, Oxford, United Kingdom) were as follows: *Fc*-receptors were blocked for 10 min (4°C) using CD16/32 (2.4G2) antibody. Cells were then surface stained with directly conjugated monoclonal antibodies including CD25 (PC61) PE and/or CD4 (GK1.5) APC-Cy7. In some experiments, 1G12 primary antibody to HEL-specific TCR (clone: 1G12; cell line kindly provided by Professor Goodnow, Australian National University) with secondary APC-conjugated anti mouse IgG1 (X56) was included. Alternatively, for a different batch of experiments, anti-Vβ8.1/8.2 TCR was used (BD BV605-conjugated; MR5-2; BD Biosciences, Oxford, United Kingdom).

For analysis of T_{reg}, cells were stained intracellularly using a FoxP3 staining kit (APC/eFluor[®] 450 conjugated FoxP3, FJK16S) according to manufacturer instructions (eBioscience, Hatfield, United Kingdom). As an additional marker for T_{reg}, folate receptor 4 antibody (anti-FR4 PerCp-Cy5.5-conjugated; 12A5, Biolegend, London, United Kingdom) was used. For detection of T cell energy, anti-CD73 (AF700-conjugated; Ty11.8; Biolegend, London, United Kingdom) was chosen. The gating strategy for the phenotypic CD4⁺ T cell characterization is provided in **Supplementary Figures 1a–f**. For intracellular cytokine staining, dissociated cells were washed and re-suspended in culture media for further *ex vivo* stimulation. Cells were incubated for 5h in RPMI medium containing 10% FBS (both from Gibco, Fisher Scientific UK Ltd., Loughborough, United Kingdom), 50 ng/ml phorbol 12-myristate-13-acetate (16) and 1 μM ionomycin (both from Sigma-Aldrich, St. Louis, MO, United States) for 5h in the presence of monensin (BD GolgiStop[™], BD Biosciences, Oxford, United Kingdom). Next, *Fc*-receptors were blocked, cells were surface stained with anti-CD4 APC-Cy7 and 1G12 antibody followed by fixation using BD Cytotfix/Cytoperm[™] (BD Biosciences, Oxford, United Kingdom). The following antibodies were used for intracellular staining: anti-mouse IFN_γ (XMG1.2) with APC; IL17A (TC11-18H10) with PE-CF594; and IL22 (1H8PWSR) with PE. In all experiments, dead cells were excluded using a dead cell exclusion dye (Fixable Viability Dye eFluor 455, eBioscience, Hatfield, United Kingdom; or eFluor 506, Biolegend, London, United Kingdom). For all flow cytometry experiments 1–2 × 10⁵ events were acquired on a BD LSRII flow cytometer (BD Bioscience, Oxford, United Kingdom). Generated data were analyzed using FlowJo[®], LLC for Windows, version 10 (TreeStar Inc., Ashland, OR, United States). Leukocytes were gated on a forward scatter (FSC-A) vs. side scatter (SSC-A) dot plot, followed by exclusion of cell aggregates using a forward scatter pulse gate (FSC-H vs. FSC-A). All subsequent analyses were based on live cells only, where unstained cells served as the gating control. Gates for individual markers of interest were set based on FMO- or isotype-controls, respectively, with acceptable background/unspecific staining signals of ≤1% of parent.

Isolation of 1G12+DN Cells

1G12+DN cells were aseptically purified from lymphoid tissues of adult 3A9 TCR mice. Spleen and lymph nodes (submandibular, superficial cervical, axillary, and inguinal LN) were collected (separately or pooled) and mechanically disrupted using 40 μm nylon cell strainers. Single cell suspensions were incubated with CD4 (L3T4) MicroBeads and the CD4⁺ cells collected, followed by a purification step. Briefly, a positive selection was performed, using magnetic bead-filled columns. Single cell suspensions from the above tissues were run through the column once, followed by 5 washes using wash buffer (3 ml each) [0.5% (v/v) bovine serum albumin (BSA), and 2 mM EDTA in Ca²⁺/Mg²⁺ free phosphate buffered saline (PBS) (all from Gibco, Fisher Scientific UK Ltd., Loughborough, United Kingdom)]. The eluted CD4⁺ cells were collected and further depleted of potentially remaining CD4⁺ contaminating cells, using a CD4⁺ T cell Isolation Kit (MACS Miltenyi Biotec, Surrey, United Kingdom), following the

manufacturer's protocol. Using flow cytometry, the purity of the 1G12+DN cell population was assessed to be around 80%.

Activation of Lymphocytes by HEL Protein and Anti-CD3/CD28 Antibodies

Activation of pooled lymph node lymphocytes from adult 3A9 mice, either with 1 μ M HEL protein (Sigma-Aldrich, St. Louis, MO, United States) or with anti-CD3 (clone 17A2)/CD28 (clone 37.51) antibodies (both USB Molecular Biology Reagents: VWR International Ltd., Lutterworth, United Kingdom) was performed as described previously (17). The lymphocytes were washed and re-suspended at a density of 0.5×10^6 cells/ml in complete medium [RPMI, 10% (v/v) FBS, 1% penicillin/streptomycin (v/v); (all from Gibco, Fisher Scientific UK Ltd., Loughborough, United Kingdom)] containing 200 pg/ml rIL-2 (Calbiochem Nottingham, United Kingdom), followed by addition of spleen feeder cells from B10.BR mice (5×10^4 cells/well). Three days later, cells were harvested and re-suspended in PBS for further use.

Adoptive Transfer

Transfer of activated, purified populations of CD4⁺ T_{conv}, 1G12+CD3-CD4⁻ (DN) T cells and unfractionated lymphocytes was prepared as outlined above and described previously (17). Cells were injected intravenously (*i.v.*; dorsal tail vein) into IRBP:HEL sTg mice of different age. EAU was clinically monitored by fundoscopy on day 5, day 8 and day 10 post-injection. After the last images had been taken on day 10, the animals were sacrificed, and eyes removed immediately for histological evaluation.

T_{reg} Cell Isolation

T_{reg} cells were aseptically purified from 3A9 TCR and dTg HEL/TCR mice aged between P50 and P70. Spleen and LN (submandibular, superficial cervical, axillary, and inguinal) were collected and pooled single cell suspensions passed through a CD4+CD25⁺ regulatory T cell isolation kit of CD4 (L3T4) MicroBeads UK followed by magnetic microbead positive and negative selection according to the manufacturer's manual. In some procedures, CD127⁺ (IL7R) T cells were removed by a further pass through a column containing CD127-antibody labeled beads as described (18). The percentage of FoxP3⁺, CD73⁺ and FR4⁺ T cells was evaluated in the purified populations by flow cytometry, and the CD4⁺ cells were found to be ~80% T_{reg}.

T_{reg} Suppression Assay

To test T_{reg} suppression activity *in vitro*, equal numbers of CFSE labeled CD4⁺CD25⁻ T_{eff} cells and mitomycin C (Sigma-Aldrich Company Ltd., Gillingham, Dorset, United Kingdom) treated antigen presenting cells (APC; 5×10^4 /well) were incubated for 3 days (5% CO₂, 37°C) with 1 μ M HEL protein (Sigma-Aldrich, St. Louis, MO, United States), and serial dilutions of purified T_{reg} ([T_{reg}:T_{eff}] ratios of [0.5:1] to [4:1]), followed by flow cytometric assessment of T_{eff} cell proliferation by evaluating progressive attenuation of CFSE staining as described previously (19).

T Cell Anergy Assay

The ability of purified CD4⁺ cells from dTg and 3A9 mice, respectively, to proliferate *in vitro* was assessed following a previously published protocol (11). CD4⁺ cells were labeled with CFSE and challenged with serial dilutions of HEL protein (10^{-5} – 10^{-11} M) in the presence of mitomycin C-treated spleen APC for 3 days, after which cell proliferation was evaluated as stated above.

Statistical Analysis

Statistical analysis was performed using GraphPad Prism for Windows, version 5 (La Jolla, CA, United States). Histograms were generated to check data distribution. For parametric data, one- or two-way ANOVA with Tukey's Multiple Comparison *post hoc* Test for inhomogeneous variances, and Student's *t*-test were used. The Mann-Whitney *u*-Test was applied on non-parametric data. Asterisks denote significant *p*-values based upon a 95% level of confidence (**p* < 0.05, ***p* < 0.01, ****p* < 0.001, *****p* < 0.0001).

RESULTS

EAU in dTg Mice Progresses From Patchy Vasculitis at P20 to Severe Retinitis at P44

We previously reported, using histological evaluation, the time of onset (P22) and incidence (100% at > P42) of spontaneous EAU in dTg mice (11). Here, using clinical fundoscopy to record global changes in the eye, we extend previous studies and more precisely time the onset of disease to P20 and fully characterize the progression of EAU in this model to peak severity of inflammation at P44 (Figure 1A, left panel and Supplementary Figure 2). In these more detailed studies, the dominant sign is inflammatory vasculitis followed by late extensive paravenous atrophy (Figure 1A, right panel and Supplementary Figure 2) and in ~30% of cases eventual phthisis bulbi (globe shrinkage) (Supplementary Figure 2, gray box). Disease is absent in P18 dTg mice but presents clinically at P20 in around 60% of mice as focal patches of vasculitis ("cuffing") of the major retinal vessels (Figure 1A and Supplementary Figure 2). By P29 all mice show signs of disease but with a range of clinical severity from small patches of retinal vasculitis to extensive vasculitis affecting all major retinal vessels and marked cellular infiltration of the vitreous gel ("vitreous haze"), obscuring retinal detail in some cases. This variable pattern continues with milder disease taking longer to reach grade 4 severity while more rapidly developing disease has begun to resolve by P44. This is accompanied by expanding areas of severe retinal atrophy particularly at sites of continuing severe vasculitis (Figure 1A and Supplementary Figure 2). By P59 active inflammation, including retinal and vitreous hemorrhage, persists in mice with slower onset disease while in more rapid onset disease, severe paravenous atrophy involving large parts of the retina has developed, with reduced inflammation mainly in the form of residual vitreous haze (Supplementary Figure 2). Retinal

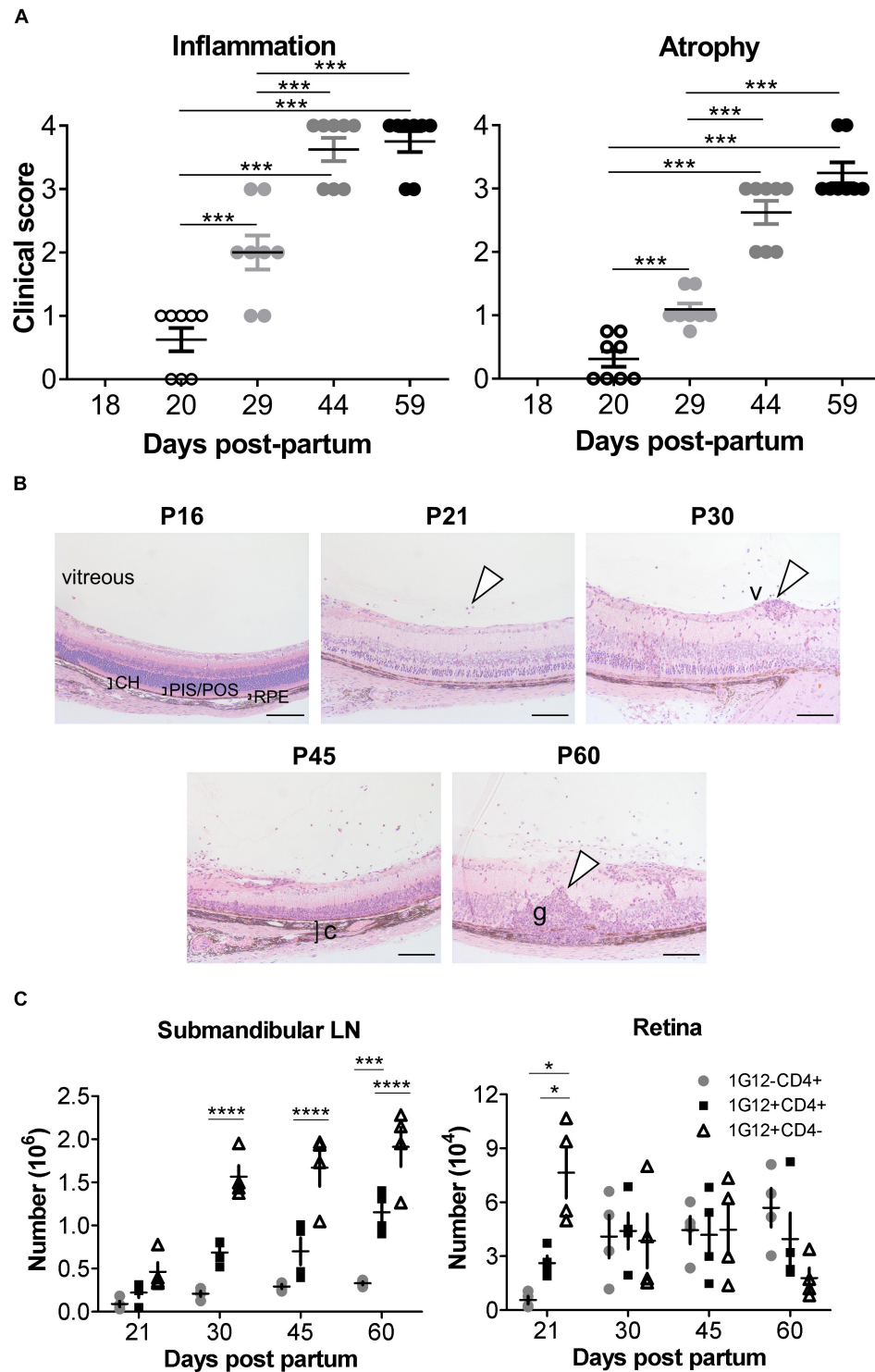


FIGURE 1 | Clinical signs and phenotypic features of ocular inflammation in dTg HEL/TCR mice. **(A)** Retinal inflammation and atrophy were scored separately according to **Supplementary Tables 1, 2**, respectively, from post-partum day P20 to P59 ($n = 8$ /group). Chronologically, atrophic changes followed the inflammatory signs. Data were analyzed using one-way ANOVA and Tukey's Multiple Comparison *post hoc* Test with $***p < 0.001$ when compared with P20 controls on a 95% level of confidence. **(B)** Eyes from dTg mice aged from P16 to P60 were fixed in 2.5% glutaraldehyde, embedded in resin, sectioned, and stained by hematoxylin and eosin (H&E). From P21, infiltrating cells were seen in the vitreous (arrowhead). From P30 to P60, vasculitis (v, arrowhead), choroiditis (c, bracket), and granuloma (g, arrowhead) were observed. CH, choroid; PIS/POS, photoreceptor inner-/outer layer; RPE, retinal pigment epithelium. Photos were taken using a ProgRes XT Core 5 color digital microscope camera (JENOPTIK Optical Systems GmbH, Jena, Germany) and mounted on a Zeiss Axioskop 40 microscope (Carl (Continued)

FIGURE 1 | Continued

Zeiss, MicroImaging GmbH, Jena, GE). Scale bar: 100 μm . Representative images are shown. **(C)** Absolute number of cells found in the submandibular/eye-draining lymph nodes (LN) and the retina, respectively, during the course of EAU in dTg mice are shown ($n = 4/\text{age group}$). The numbers of 1G12+ double negative (DN), 1G12+CD4+ and non-antigen-specific CD4+ T cells increased steadily with age in dTg mice. The first cells populating the eye-draining LN and retinas of dTg mice were mostly 1G12+DN. The numbers of 1G12+DN cells decreased with age in the retinas of dTg mice, whereas non-antigen-specific (naïve) CD4+ increased in the later stage of EAU. Data were analyzed using one-way ANOVA and Tukey's Multiple Comparison *post hoc* Test with $*p < 0.05$, $***p < 0.001$, $****p < 0.0001$ on a 95% level of confidence. Cell numbers are the average of 4 pairs of retina or DLN, i.e., cell count/pair. 1×10^5 total events were recorded. Total numbers provided were extrapolated based on total cell counts, determined using a Coulter cell counter prior to sample processing.

atrophy is accompanied with “pipe-stem” sheathing and severe “straightening” of the retinal vessels (**Supplementary Figure 2**, white arrowhead).

The two major manifestations of disease (inflammation and atrophy) were sufficiently different to merit a dual grading scheme (**Supplementary Tables 1, 2**). Atrophic retinal changes generally occurred at sites of resolving vasculitis accounting for the paravenous distribution, which spread to involve large areas of retina (**Figure 1A** and **Supplementary Figure 2**). The atrophic changes occurred with a slightly slower kinetic than the inflammatory disease (**Figure 1A** and **Supplementary Figure 2**).

In these experiments, we precisely pinpointed the clinical signs of EAU to progress from patchy vasculitis at P20, to severe retinitis at P44 (gradually leveling-off thereafter) and affecting dTg mice with a 100% incidence.

Double-Transgenic HEL/TCR Mice Retain Lymphopenia Throughout Adulthood

The next experiments further defined the exact phenotype of our dTg mice focusing on the progression of their inherent T cell thymic clonal deletion over time. We previously reported, dTg mice are profoundly lymphopenic compared to 3A9 TCR mice (11), affecting particularly the CD4+ T cell compartment (**Supplementary Figure 3** and **Table 3**). At P21 the percentage of CD4+ T cells is $\sim 4\%$ in dTg mice compared to $\sim 25\%$ in 3A9 mice. In time, there is gradual expansion in CD4+ populations, but in dTg mice lymphopenia persists to P60 ($\sim 20\%$ cells in dTg vs. $\sim 45\%$ in 3A9 mice; end of observation) (**Supplementary Figure 3**). Despite the very low T cell numbers in P21 dTg mice, EAU onset occurred at this time as seen both clinically (**Figure 1A** and **Supplementary Figure 2**) and histologically (**Figure 1B**). Since EAU in dTg mice is due to CD4+ HEL-specific T cells (11), we asked what percentage of T cells in lymphopenic dTg mice were HEL-specific and how many HEL-specific T cells infiltrated the retina.

HEL-specific T cells express the V β 8.2 TCR chain in the 3A9 TCR mouse and can be identified using the 1G12 monoclonal antibody (20). We found that the 1G12 antibody also detects a DN CD3+CD4-CD8- T cell population. In the eye-draining lymph nodes (DLN) of dTg mice at all stages of disease, the 1G12+DN population was consistently greater than the 1G12+CD4+ population. The 1G12+CD4+ population also increased with time but remained significantly lower than the total 1G12+CD4- T cell population (**Figure 1C**), as previously reported in other models (21, 22). In the retina, DN cells formed the greater part of the early T cell

infiltrate at onset of disease (P21: $\sim 7.5 \times 10^4/\text{retina}$) but declined steeply in number by P30 and were infrequent at P60 (**Figure 1C**). Conversely, 1G12+CD4+ T cells, were considerably less frequent at onset of disease (P21, $\sim 3.0 \times 10^4/\text{retina}$) but increased and remained stable in absolute numbers to P60. Non-antigen-specific 1G12-CD4+ T cells also increased through P60 and became the most frequent cell type in the retina by that time (P60, $\sim 6 \times 10^4/\text{retina}$) (**Figure 1C**). These data suggest selective recruitment/accumulation of antigen-specific CD4+ T cells over time. We hypothesize that the prominent infiltration of DN T cells identified at the onset of disease may facilitate later accumulation of CD4+ T cells by initiating breakdown of the blood-retinal barrier.

Retinal Granulomas Are Abundant in dTg Mice and Resemble Tertiary Lymphoid Organs

Immuno-histological examination of the retina provided further insight into the behavior of DN vs. CD4+ T cells in the retina. As shown by fundoscopy (**Figure 1A**), EAU is characterized by patches of focal inflammation which on histology present as focal granulomas separated by areas of normal retina (**Figure 1B**). However, by immunohistochemistry, apparently normal retina is initially infiltrated by small numbers of single CD4+ T cells in the inner and outer nuclear layers in contact with HEL+ photoreceptor membrane (**Figure 2Aa,b**). Damage to the outer segments was associated with F4/80+ macrophage infiltration into the subretinal space (**Figure 2Ac**), a characteristic early sign of EAU (23). With more severe disease, large swathes of retina had entirely lost HEL protein expression and were replaced by dense granuloma formations, while the neighboring less infiltrated retina remained HEL+ (**Figure 2Ad**). Triple confocal staining revealed that inflammatory granulomas contained several cell types including CD3+CD4+ dual-staining T cells, CD3+CD4- single-staining T cells (presumed DN cells), F4/80+ macrophages, CD11b+ and CD11c+ myeloid cells and B220+ B cells, and had features of TLO (24) (**Figure 2Ae-l**). Multiple granulomas were typically found in a single section of retinal tissue, the number and extent increasing with time. Closer examination revealed the presence of MHC Class II++ CD11c++ presumed DC (25) in the interstices of the TLO-like masses, and in close contact with many CD4+ T cells (**Figure 2Aj**). In contrast, CD3+CD4- (DN) T cells appeared to congregate in B cell-rich areas (**Figure 2Ak,l**). In summary, inflamed retinas of dTg mice presented with granulomas

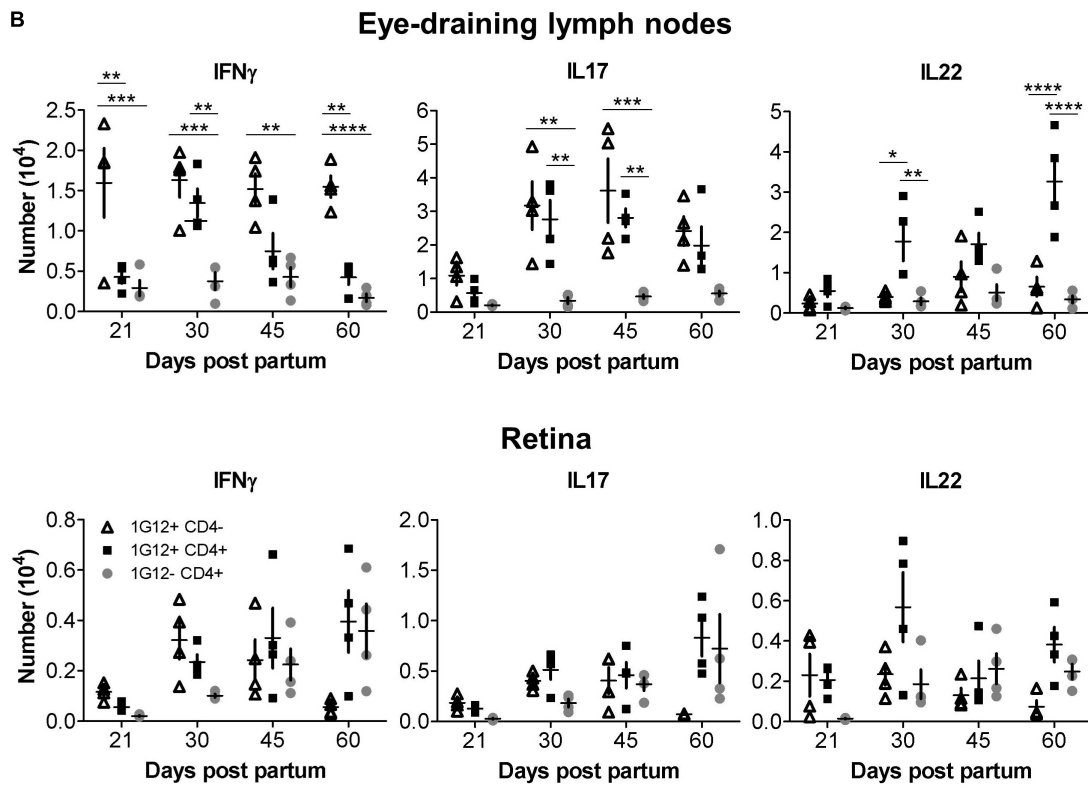
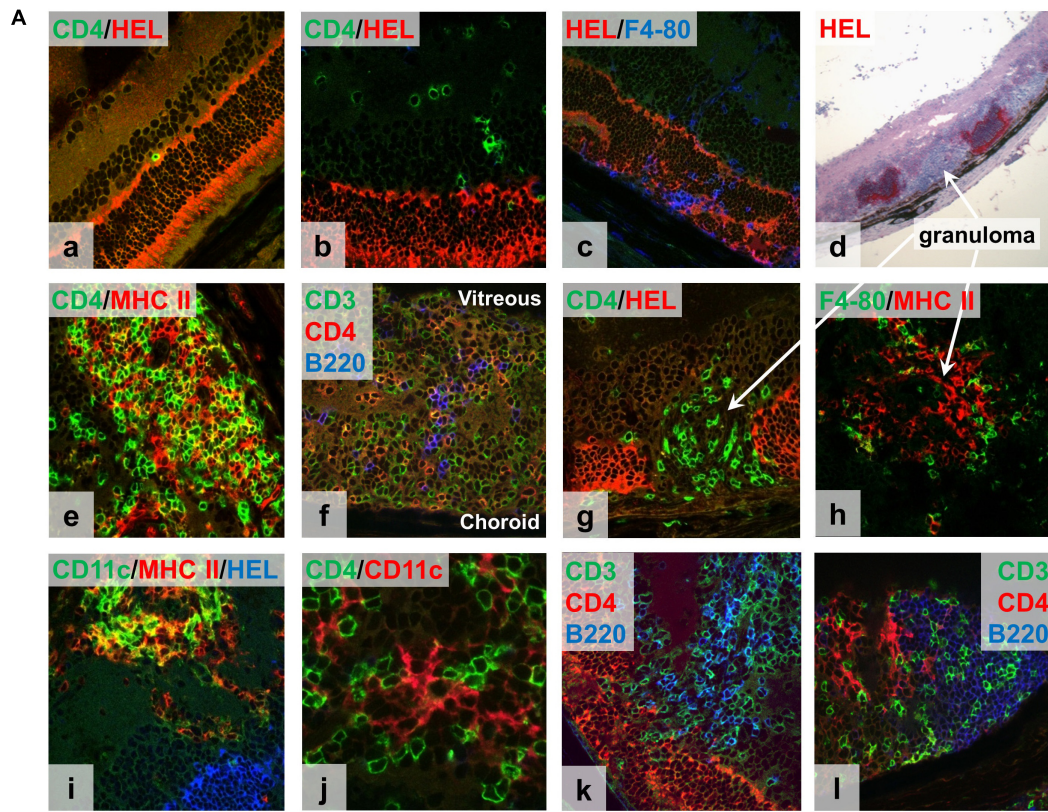


FIGURE 2 | Continued

FIGURE 2 | Immunohistology and intracellular cytokine analysis (IFN γ , IL17, and IL22) of eye-draining lymph node- (DLN) and retina-infiltrating cells over the course of spontaneous EAU in dTg HEL/TCR mice. **(A)** Representative confocal fluorescent **(a–c,e–l)** and light microscopic **(d)** immunohistochemistry of frozen retinal sections from (P24) dTg HEL/TCR mice are shown. Sections are representative of initial retinal inflammatory changes **(a–c)** and advanced retinal inflammatory damage **(d–l)**. Infiltrating cells identified include: **(a,b,f,k,l)**, CD3+CD4+ double-stained T cells, CD3+CD4- single-stained, presumed double-negative (DN) T cells; **(c,h)**, macrophages (F4/80+); **(e,i)**, MHC class II+ and CD11c+ (presumed DC); and **(f,k,l)**, B cells. In panels **(d,g,h)** granulomas are shown. In panels **(f,k,l)**, granulomas have features of tertiary lymphoid organs (TLO). Areas of retinal HEL protein expression were identified using a polyclonal HEL-specific antibody. The slides were mounted with Hydromount™ Aqueous Non-fluorescing Mounting Media (National diagnostics, Hull, United Kingdom), and were examined with a Zeiss LSM510 confocal microscope (Carl Zeiss Meditec, Göttingen, Germany). **(B)** Flow cytometric analysis of intracellular cytokine expression in lymph node cell populations at different stages of EAU development. Single cell suspensions were prepared from eye-draining lymph nodes (upper panel) and retinas (lower panel), respectively ($n = 4$ /age group). Flow cytometric analysis of intracellular cytokine expression by three different T cell populations (1G12+CD4-, 1G12+CD4+, and 1G12-CD4+) at different time points during evolution of EAU in dTg mice was completed. Upper panel (dTg DLN): at disease onset (P21), only small numbers of antigen-specific CD4+ cells gave a positive signal for intracellular cytokines; a gradual up to fivefold increase was found by P30. Significantly fewer IFN γ -secreting antigen-specific CD4+ T cells (declining further toward P60) than IL17+ and IL22+ cells were found. In contrast, levels of IL17+ cells were sustained in the DLN through P60. IL22 expression was also sustained and increased in CD4+ but not DN HEL-specific T cells through P60. CD4+ non-antigen-specific T cells (1G12-) were low for all three cytokines over the course of the observation. Lower panel (dTg retina): Cytokine expression by cells mirrored those changes found in the DLN except at P45 when there were proportionately more non-antigen specific IL22+CD4+ T cells found in the retina. By P60 non-antigen-specific CD4+ T cells in the retina expressed similar levels of IL22 and IL17 as antigen-specific cells, which suggests some level of bystander activation. Cells had been stimulated with 50 ng/ml PMA and permeabilized with 1 μ M ionomycin for 5 h in the presence of monensin (BD GolgiStop™, BD Biosciences, Oxford, United Kingdom). The cells were surface labeled for CD4 and 1G12 (3A9 TCR) followed by intracellular cytokine labeling for IFN γ , IL17 and IL22. 1×10^5 events/sample were acquired on a BD LSR II flow cytometer. Data were analyzed for each specific time point using one-way ANOVA and Tukey's Multiple Comparison *post hoc* Test with * $p < 0.05$, ** $p < 0.01$, *** $p < 0.001$, **** $p < 0.0001$ on a 95% level of confidence. Cell numbers are the average of 4 pairs of retina or DLN, i.e., cell count/pair. 1×10^5 total events were recorded. Total numbers provided were extrapolated based on total cell counts, determined using a Coulter cell counter prior to sample processing.

closely resembling TLO containing an abundance of diverse pro-inflammatory cell types with strong antigen-presenting activity fostering uveitogenesis.

IL17 Is the Predominant Cytokine in CD4+ and DN HEL-Specific T Cells During EAU, CD4+ IL22-Expressing T Cells Dominate Late Stage Disease

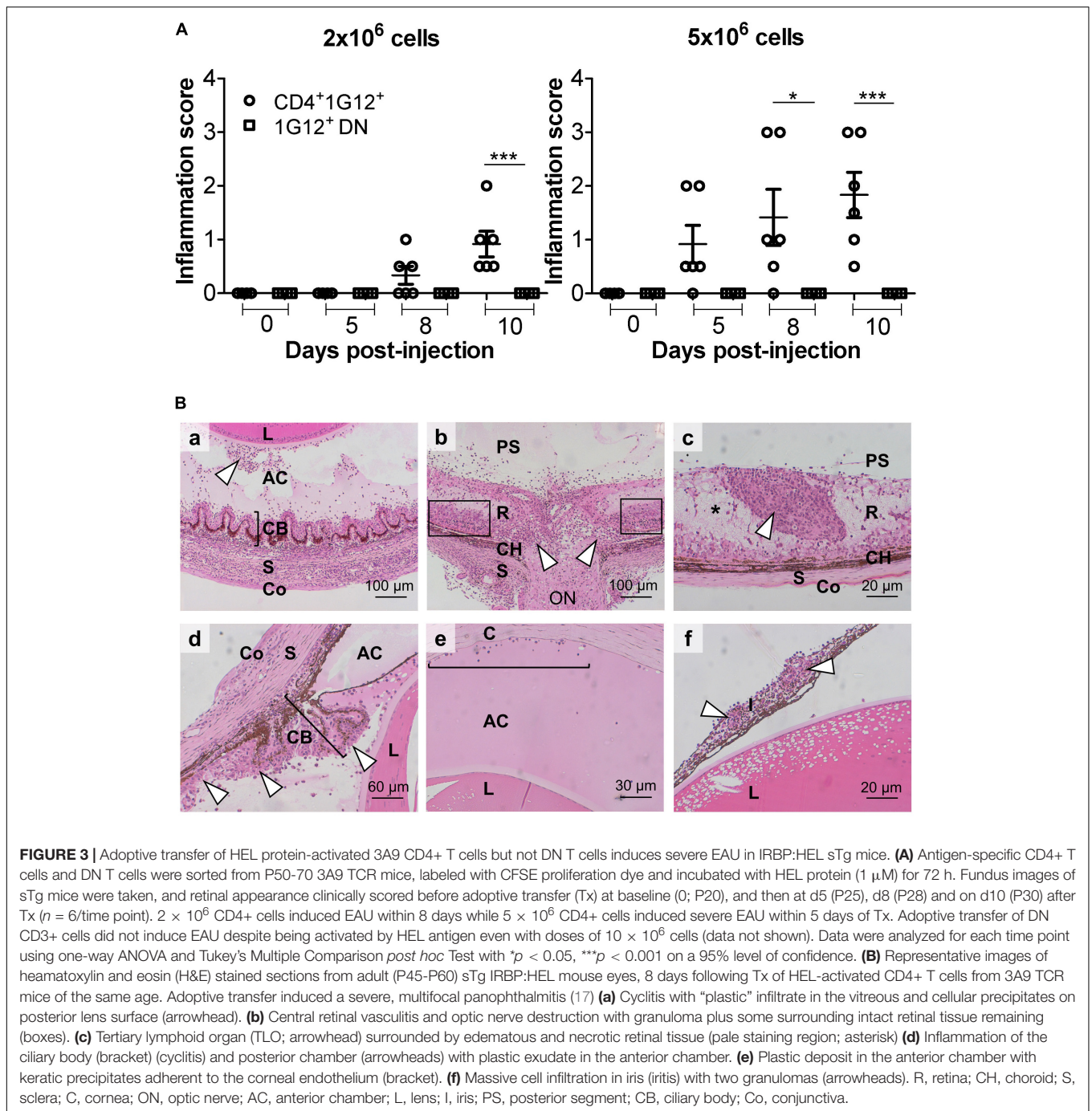
Both Th1 and Th17 have been implicated in the pathogenesis of EAU (26, 27). We therefore evaluated the production of these cytokines during the course of EAU in the dTg mice (gating strategy for flow cytometric analysis provided in **Supplementary Figures 4a–d**). Since both IL22 and IL17 are produced by lymphoid tissue-inducer cells (LTi cells) involved in the generation of TLO [reviewed in Pipi et al. (28)] we further assessed IL22 production in dTg mice. In the lymphopenic dTg eye DLN, very small numbers of antigen-specific CD4+ T cells were positive for intracellular cytokines ($\sim 0.5 \times 10^4$) at the onset of disease (**Figure 2B**, upper panels) but gradually increased up to fivefold to peak levels at P30. IFN γ -secreting antigen-specific CD4+ T cells were significantly fewer in number than IL17+ and IL22+ cells and gradually declined by P60. In contrast, levels of the IL17+ cells in the antigen-specific CD4+ and DN T cell populations were sustained in the DLN through P60. In contrast, IL22 expression was sustained and even increased in CD4+ but not DN HEL-specific T cells through P60. CD4+ non-antigen-specific T cells (1G12-) secreted low levels of all three cytokines for the duration of the disease. Cytokine expression by cells infiltrating the retina mirrored the changes in the DLN except at P45 when there appeared to be proportionately more non-antigen specific IL22+CD4+ T cells in the retina (**Figure 2B**, lower panels). In addition, by P60 non-antigen-specific CD4+T cells in the retina expressed similar levels of IL22 and IL17 as

antigen-specific cells, suggesting some level of bystander activation (**Figure 2B**, lower panel).

HEL-Specific CD4+ T Cells Induce EAU on Adoptive Transfer but Require Prior Activation With Cognate Antigen

It was imperative to determine which T cell subset(s) induced EAU in dTg mice, and to test this antigen-specific CD4+ and DN T cells were separately isolated from P50-70 3A9 mice using magnetic bead technology (see Methods), further enriched, and adoptively transferred to P21 IRBP:HEL sTg mice. Prior analysis showed that both subsets of T cells proliferated *in vitro* in response to HEL protein, with DN cells responding less strongly (**Supplementary Figure 5A**). Adoptive transfer of $1-2 \times 10^6$ HEL-activated CD4+ T cells was sufficient to induce EAU 8 days after transfer while 5×10^6 CD4+ cells induced severe EAU 5 days after transfer both clinically (**Figure 3A** and **Supplementary Figure 5B**) and histologically (**Figure 3B**). Disease induction required *in vitro* activation of the T cells with HEL protein (1 μ M) while non-specific activation with anti-CD3/CD28 antibody failed to induce EAU (17) (**Supplementary Figure 5B**). In contrast to HEL-activated CD4+ T cells, HEL-activated antigen-specific DN cells failed to induce disease at any time up to 10 days after Tx (**Supplementary Figure 5B**).

We next asked the central question of whether the level of retinal HEL expression determined the animals' susceptibility to EAU (29) after Tx of activated antigen-specific CD4+ T cells. If this were the case, this finding would explain the model's high level of antigen-specificity in EAU induction. We have shown in a companion paper series that the levels of HEL expression decline in sTg mice as retinal degeneration develops with age (12, 30). We therefore adoptively transferred 4.5×10^6 CD4+ T cells to sTg mice of increasing age. Severe inflammatory disease was observed in mice of 3 weeks of



age (P21) while minimal inflammation was found in mice aged 6–8 weeks old (P42-56) (**Supplementary Figure 6A**). No inflammation was observed in mice aged >8 months (>P240), and no disease at any age of mice was induced using CD3/CD28-activated antigen-specific T cells (**Supplementary Figure 6B**) (17). In conclusion, these data point toward a dose-related induction of EAU dependent on the level of HEL expression in the retina. A key observation was that the levels of retinal atrophy were similar in mice receiving HEL-activated T cells or anti-CD3/CD28 activated T cells indicating that the atrophic

changes in this model are not antigen-specific (**Supplementary Figures 6C,D**).

Lymphopenic dTg Mice Show Limited T Cell Anergy and Have Reduced Numbers of T_{reg}

In exploring the mechanism of how T cell mediated EAU in dTg mice develops spontaneously, we had found evidence for limited T cell anergy in preceding work (11). Here, we report

in detail that HEL-specific T cells in dTg mice indeed display a limited level of anergy since they proliferated *in vitro* in response to low levels of HEL, albeit less strongly than 3A9 control T cells (Figure 4). Total CD4⁺ cells from 3A9 and dTg mice were purified by negative selection and stimulated *in vitro* with varying amounts of HEL in the presence of mitomycin C-treated APC for three days (Figure 4). The proliferative response of dTg CD4⁺ T cells to high levels of HEL antigen was similar to that of 3A9 TCR controls. However, when exposed to a middle range of HEL (10^{-7} M to 10^{-9} M), the proliferative response of dTg CD4⁺ T cells significantly dropped compared to 3A9 CD4⁺ T cells (Figure 4). A significant reduction of proliferation was seen in dTg CD4⁺ T cells at even lower concentrations of HEL (10^{-10} and 10^{-11} M) (Figure 4). In demonstrating some level of proliferative response, dTg T cells appear different from the fully anergic T cells of similar transgenic Ins-HEL mice (21, 31) and thus have the potential to be constitutively activated *in vivo* if exposed to cognate antigen.

In our experiments we also found that T_{reg} numbers in dTg lymphopenic mice in the eye DLN were very infrequent ($\sim 2 \times 10^3$), and in the retina were minimal ($< 1 \times 10^3$) at the time of disease onset (P21) (Figures 5A,B and Supplementary Table 4). We therefore re-considered the possibility that, in addition to a relative failure of T cell anergy, deletion of T_{reg} may have contributed to EAU development allowing uncontrolled expansion of uveitogenic IL17⁺/IL22⁺ or IFN γ ⁺ T cells. During the course of disease (up to P60; end of observation) the number of T_{reg} in the DLN increased but never reached levels equivalent to non-Tg or 3A9 mice (Figure 5A). However, they appeared to be more effective in suppressing T cell proliferation *in vitro*

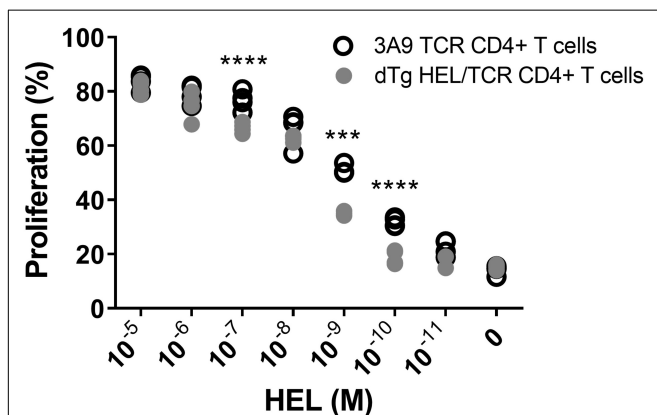


FIGURE 4 | *In vitro* evidence suggests limited anergy of CD4⁺ cells in dTg HEL/TCR mice. CD4⁺ T cells isolated from 3A9 TCR or dTg HEL/TCR mice aged P50-P70 (in the presence of mitomycin C-treated antigen-presenting feeder cells from B10.Br WT mice) were incubated with decreasing concentrations of HEL protein (10^{-5} – 10^{-11} M over 72 h), and their proliferation assessed using flow cytometry to measure CFSE dilution. Limited anergy of dTg HEL/TCR CD4⁺ T cells (i.e., reduced specific responsiveness to HEL reflected in consistently low proliferation) was observed at and below a HEL antigen concentration of 10^{-10} M. Significant differences were assessed using one-way ANOVA, followed by Tukey *post hoc* test with $***p < 0.001$, $****p < 0.0001$ on a 95% level of confidence. The experiment was independently repeated twice.

(Figure 5C). Notably, the number of T_{reg} in the retina of dTg mice increased significantly during this period (Figure 5B; gating strategy for detection of T_{reg} provided in Supplementary Figures 7a,b) which coincided with stabilization and resolution of inflammation in the eye (Figure 1 and Supplementary Figure 2). Similar results were obtained when comparing retinas of P33 dTg vs. 3A9 TCR mice in terms of non-pathogenic cell populations. While in the eye DLN, the distribution pattern of those cell populations of interest were highly similar between the genotypes, there was a clear increase in T_{reg} and T_{an} in retinas of dTg mice, compared to their 3A9 counterparts (Figure 6).

Limited Anergy vs. Reduced T_{reg} in EAU Pathogenesis in dTg Mice

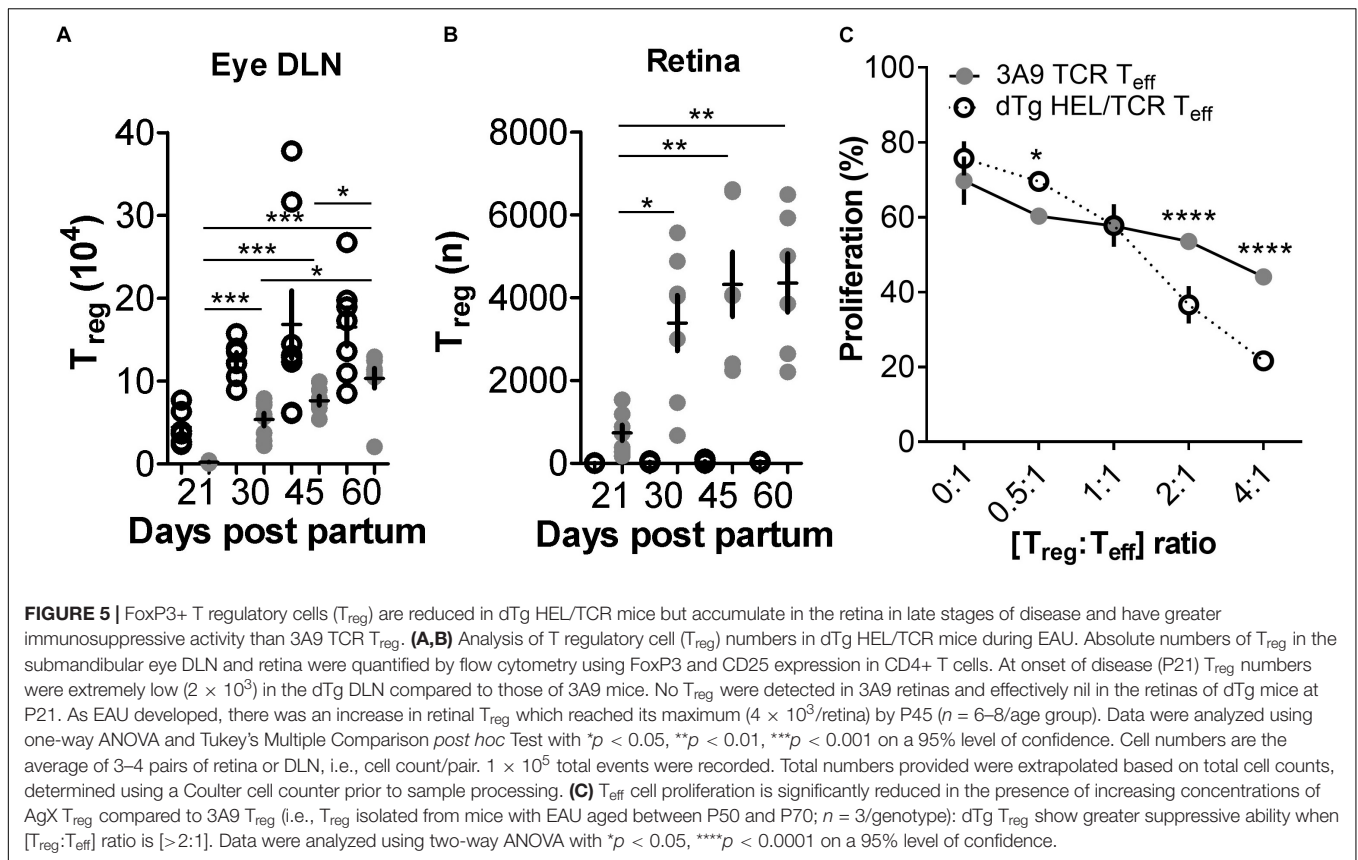
Recent studies have suggested that generation of T_{an} and T_{reg} may under certain conditions be a reciprocal process (1, 32). Since we have found that both limited anergy and lack of T_{reg} potentially contributed to development of EAU in dTg mice, we explored the phenotype of these T cell populations at a single time point (P33) when EAU severity is approaching peak levels (Figure 1). Anergic T cells were identified as CD25⁺FoxP3⁻CD73⁺FR4⁺ cells, while T_{reg} were identified as CD25^{hi}FoxP3⁺FR4[±] (33, 34) and their relative proportions within the AgX population of P33 mice with EAU and in 3A9 mice were compared (Figure 6).

Unfractionated DLN CD4⁺ T cells in P33 3A9 mice contain $\sim 33\%$ CD25⁺FoxP3⁻ effector cells, of which 83% are V β 8.1/8.2+ [antigen-experienced (35)] (Figure 6A). Approximately 7% T_{reg} cells are also present in the DLN CD4⁺ T cell population, all of which were HEL-specific. In addition, there were $\sim 0.5\%$ T_{an} cells indicating that there is some degree of overlap between these two populations of T cells (Figure 6A). In the P33 3A9 retina, there were few T cells (Figure 6B) probably representing contaminating intravascular cells.

Unfractionated cells in the DLN of the lymphopenic dTg mice at P33 contained a significant proportional increase in T_{reg} (up to $\sim 18\%$) as well as T_{an} cells (up to $\sim 2\%$) although the absolute number of T_{reg} and T_{an} were the same as in 3A9 mice. Proportionally there were nearly twice as many T_{reg} and T_{an} in the DLN of dTg mice compared to 3A9 mice. In the retina of P33 dTg mice, there were up to 20% T_{reg} while T_{an} accounted for 8% of the CD4⁺ T cell population indicating similar [T_{reg}:T_{eff}] and [T_{reg}:T_{an}] ratios as in the dTg DLN (Figures 6C,D).

Antigen-Experienced CD4⁺FoxP3⁺ T_{reg} Arrest EAU Development in dTg HEL/TCR Mice

Our data propose that the proportional increase in T_{reg} in the retina (Figure 6B vs. D) might promote resolution of EAU which was found to stabilize at $\sim P44$ –59 and gradually burn out (Figure 1 and Supplementary Figure 2). We therefore asked whether Tx of AgX T cells, i.e., cells from mice at peak to late stages of disease/disease resolution, which would contain increased numbers of T_{reg} (~ 18 –20%) (Figure 6), might prevent development of disease if they were administered at time of disease onset (P20). To this end, initial pilot experiments



were performed with unfractionated T cells and histological assessment only (Figure 7A). While Tx of naïve (3A9) T cells had no effect on disease progression, cells from dTg mice (AgX cells) completely prevented development of EAU (Figure 7A). Importantly, the transferred cells had not been activated by HEL antigen *in vitro* prior to Tx. Next, Tx experiments were performed using purified cell populations and clinical grading of EAU. Adoptive transfer of both FoxP3+CD25^{hi}CD127+ and FoxP3+CD25^{hi}CD127- T_{reg} from dTg mice but not from 3A9 mice prevented development of EAU and in some cases reversed disease (Figures 7B,C and Supplementary Figure 8). In stark contrast, Tx of FoxP3-CD4+CD25-CD127+ T cells did not significantly alter progression of disease (Figure 7D). Phenotypic analysis of the T_{reg} population within the immunosuppressive antigen-experienced T cells is summarized in Table 1. The representative data shown attest to a FoxP3+, non-Tr1 T_{reg} type.

DISCUSSION

We report here new data in a previously described model of spontaneous experimental autoimmune uveoretinitis (EAU) generated by cross-breeding IRBP:HEL sTg mice (sTg) with 3A9 TCR mice to produce dTg HEL/TCR (dTg) mice (11). In a companion paper series (12, 30), we showed that insertion of the HEL gene in B10.BR wild type mice to create the sTg mice, induces a non-inflammatory, mild to moderate retinal

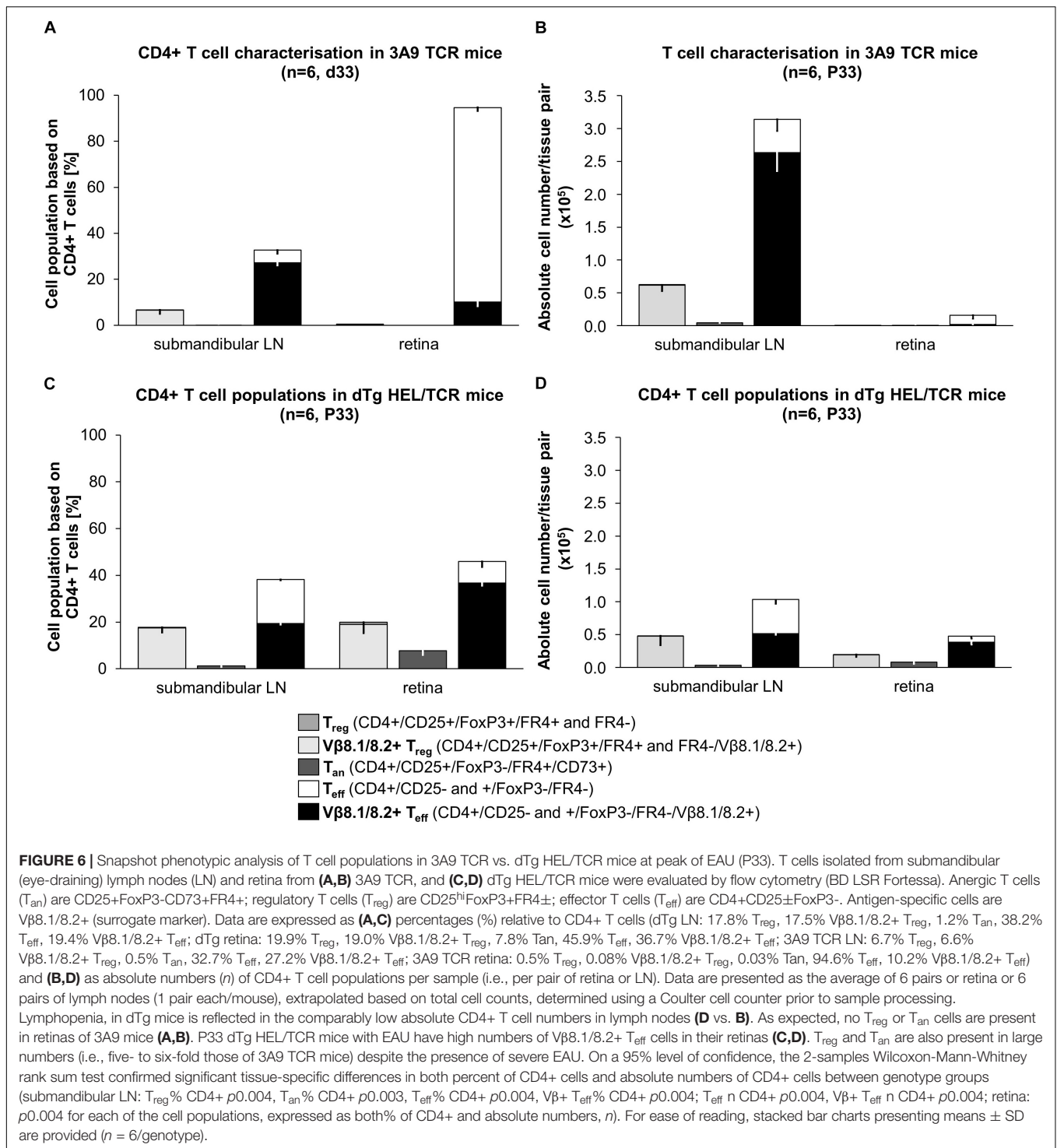
TABLE 1 | Phenotype of immunosuppressive, antigen-experienced T_{reg}.

Pre-CD4+ enrichment	
Marker	Percent within T _{reg} cells (CD4+CD25+FoxP3+)
Eomes+	0.5
Helios+	70.0
CD127+	15.0
LAG3+	1.0
Post-CD4+ enrichment	
Eomes+	0.0
Helios+	97.0
CD127+	0.8
LAG3+	0.3

Flow cytometric characterization of CD4+CD25+FoxP3+ T_{reg} cells obtained from dTg HEL/TCR mice, pre- and post-magnetic bead CD4+ enrichment. Representative data are provided.

degeneration with photoreceptor shortening. This is associated with a relative reduction in the amount of IRBP in the retina, an essential retina-specific protein for normal photoreceptor health (36). The retina is otherwise normal particularly in the early post-natal period and sTg mice do not develop uveitis.

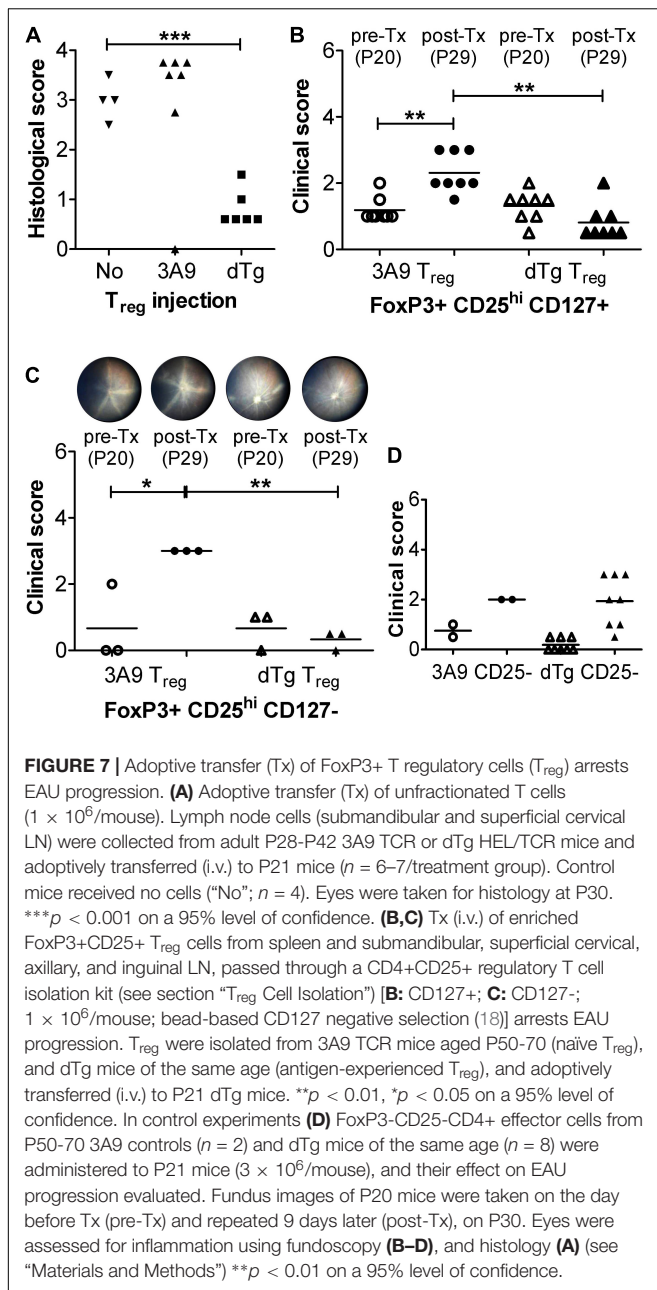
In the present study, dTg mice develop signs of retinal inflammation (vasculitis and granulomatous disease) in a patchy focal distribution, at several sites in the fundus, as early as P20



which progresses rapidly to involve the entire retina. There is slight variability with regard to the time of onset of the disease and ultimate severity, but by P44 100% of mice have severe (grade 3–4) signs of EAU. In addition, there is associated retinal atrophy which culminates in extensive loss of retinal tissue and in some mice (30% of mice by P90) progresses to involve the entire globe (phthisis). The disease thus resembles severe progressive chronic

ocular inflammatory disease in humans (autoimmune uveitis) in several aspects including long-term globe shrinkage (37).

3A9 TCR mice contain around 70% HEL-specific CD4⁺ T cells in the peripheral lymphoid tissue, >90% of which express a Vβ8.2 TCR and can be directly identified using a specific antibody against Vβ8.1/8.2 (11, 38). Flow cytometric analysis of eye DLN cells in dTg mice indicated there was extensive



thymic deletion of T cells in the early stages of disease (P20), which affected HEL-specific CD4+ T cells particularly. Peripheral lymphoid tissues were populated predominantly with a second HEL-specific population of DN T cells (CD3+CD4-CD8-) and remained so for at least 60 days when this part of the study was concluded. In the eye DLN, CD4+ HEL-specific T cells increased in frequency as the disease progressed but less so in non-eye DLN (data not shown). Since HEL antigen is expressed in the thymus (11) and in the peripheral lymphoid tissues (29) in sTg mice, HEL-specific CD4+ T cell deletion in dTg mice is predictable. In similar models, skewing of the peripheral T cell population toward DN T cells is well recognized and considered to be characteristic of some dTg TCR models (39).

DN T cells were also the most frequent T cell in the retinal cell infiltrate at the onset of inflammation. However, during progression of the disease they became less frequent while the numbers of CD4+ HEL-specific T cells remained constant. In addition, IL17 and IL22-expressing CD4+ HEL-specific T cells were more frequent and consistent than DN and non-HEL-specific endogenous T cells. Both CD4+IFN γ + and IL17+ T cells are recognized as pathogenic in conventional models of EAU [reviewed in Lee et al. (40)] and if pathogenicity can be attributed to specific cytokines, IFN γ + and IL17+ DN cells in this model would certainly be considered pathogenic. However, in the dTg HEL/TCR mouse reported here, the predominant CD4+ T cells which are pathogenic were IL17 producers, as revealed by Tx experiments to sTg mice. Despite the fact that both the CD4+ T cells and DN T cells respond to HEL protein *in vitro* this is particularly remarkable. In fact, endogenous non-HEL-specific T cells may play a more significant role than DN T cells in the dTg model, since they become the dominant cell in the late stages of disease, and Rag-/- dTg mice do not develop EAU (11). This also raised the central question of whether the amount of HEL antigen expressed in the retina influences the degree of the inflammatory response it triggers. We have shown that sTg mice, which develop an age-related photoreceptor degeneration with reduced levels of HEL expression (12), become less susceptible to HEL-activated 3A9 CD4+ T cell-induced EAU. The precise role the DN T cells play in this model is not clear. The CD4 molecule is known to significantly amplify T cell responses [reviewed in Huppa et al. (41)] which may partly explain the lack of DN T cell pathogenicity *in vivo*, although DN cells respond well to HEL *in vitro*. In addition, the process of generation of transgenic $\alpha\beta$ TCR appears to disrupt later expression of $\gamma\delta$ TCR as well as the CD8 molecule, and it can be surmised that it also affects proper expression of the CD4 molecule (42, 43). Other possibilities can be envisaged. Previous studies have suggested that a subset of CD3+CD4- T cells may actually have an immunoregulatory role (44) but it may also be that, in the current model, the frequency of DN T cells is simply a response to the vacated lymphopenic space (45) generated by the extensive thymic deletion.

The data thus confirm that the pathogenic T cell in this model is the CD4+ T cell. In addition to IFN γ and IL17, CD4 T cells, but not DN T cells, expressed increasing levels of IL22 into the late stages of the disease in the DLN. In the retina, IL22 was expressed by both CD4+ HEL-specific T cells and endogenous CD4 T cells, but not DN cells. This correlated with the immunohistochemical change from a pauci-cellular infiltration of CD4+ T cells and myeloid cells in the photoreceptor layer to the development of large full thickness granulomas containing many cell types, including B cells, with the characteristics of tertiary lymphoid organs (TLO). These are considered to be sites where active local antigen presentation by DC occurs in the inflamed tissue and have been previously observed in a Tg IRBP-TCR model of EAU (46). IL22 is known to be involved in lymphoid tissues inducer type cells (47) *in situ* and both IL22 and IL17 are implicated in the formation of TLO (15, 48). These data fit with IL22+IL17+CD4+ T cells being primarily pathogenic in this model with a secondary contribution from the endogenous T cell populations. Most recently, however, IL22 has been shown to have a regulatory effect

on retinal inflammation when administered locally, indicating that its precise role in this model is not yet defined (49).

The mechanism whereby tolerance is broken, and spontaneous autoimmunity develops in dTg mice was attributed, in a related preceding study, to reduced T cell anergy (11). The suggestion that lymphopenia might drive the susceptibility to antigen-specific EAU is supported by previous work from Gregerson's lab who showed that adoptive transfer of beta-galactosidase TCR specific (bgalTCR) T cells, even when activated *in vitro* prior to transfer, failed to induce EAU in mice expressing bgal under control of the promoter for retinal arrestin (arrbgal mice). In addition, bone marrow chimeric adult arrbgal mice failed to develop EAU. However, mice rendered lymphopenic developed EAU when they were adoptively transferred with bgal+ TCR T cells depleted of T_{reg} (CD25+ T cells). Thus, the combination of lymphopenia-induced reduction in the numbers of endogenous T_{reg} plus depletion of exogenous T_{reg} from the adoptive T_{eff} cell population, allowed the development of severe EAU (50). The data in the current paper support this view since spontaneous disease develops when the mice are profoundly lymphopenic, and particularly in the T_{reg} compartment (Figure 5). The current work also takes it to the next level by showing that adoptive transfer of a population of antigen-experienced, T_{reg}-containing CD4+ T cells, can prevent lymphopenia-associated spontaneous EAU in dTg HEL/TCR mice.

We also explored T_{reg} function *in vitro* and while there was some evidence for greater proliferation of CD4+CD25+ T_{reg} from dTg mice, T_{reg} measured in the thymus and spleen were not significantly different nor could we generate any convincing *in vivo* evidence for a T_{reg} effect using ML5 recipients (11). Hence, the question of an additional defect in T_{reg} function in this model was left open. In the present study, we revisited this question. We first confirmed that CD4+ T cells from dTg mice with EAU were not fully anergic as has been reported, for instance, for Ins-HEL CD4+ T cells (21) although they responded less well to low doses of HEL *in vitro* than 3A9 CD4+ T cells. We next re-explored the role of T_{reg}. As for the overall T cell population, CD4+CD25+FoxP3+ T_{reg} underwent extensive thymic deletion in the early postnatal period and although they gradually increased in the eye DLN to P60, they were consistently reduced in number compared to non-Tg WT mice (data not shown) and to 3A9 control mice (Figure 5A). It thus appeared that both limited anergy and reduced T_{reg} numbers contributed to development of autoimmunity in this lymphopenic model of EAU. Recently it has been shown that there is a reciprocal relationship between T_{reg} (CD25^{hi}FoxP3+FR4±) and T_{an} (CD25+FoxP3-CD73+FR4+) cells (32, 33). We therefore explored this relationship in the dTg model at a single time point of peak disease and found that while the proportions of T_{reg} and, less so, of T_{an} in the DLN of dTg mice were greater than in the DLN of 3A9 mice, the absolute numbers were similar in both DLN. Unlike T effector cells (CD25-/+), they were 100% HEL-specific. In contrast, in the inflamed retina of dTg mice, the relative and absolute proportions of T_{an} were greater than in the DLN, suggesting that there was a

higher trend toward T_{an} than T_{reg} generation at the site of tissue damage. Which of these two populations is the more effective in terms of suppressing disease is unclear, but our *in vitro* studies indicated that, in the context of T_{reg}, antigen-experienced dTg T_{reg} are more effective than naïve 3A9 T_{reg}.

Gregerson's group have made a strong case for T_{reg} generation locally, based in part on the lack of bgal expression in the thymus as well as local depletion studies using DTR/GFP mice crossed to the arrbgal mice (51). Our data support this concept to some extent, as we suggest that T_{eff} may become T_{an} and convert to T_{reg} *in situ* in the retina during EAU progression (Figure 6). However, the development of spontaneous EAU in the current model is likely to be mostly due to a failure of thymic T_{reg}, not only because HEL is expressed in the thymus (11) but because of the profound lymphopenia and virtual absence of T_{reg} from the onset of disease at P21 (Figure 5).

We therefore decided to directly compare dTg antigen-experienced T_{reg} with 3A9 T_{reg} *in vivo*. We hypothesized that the small numbers ($\sim 0.7 \times 10^3$) which were detected in the retina at P21 and gradually increased to $\sim 4 \times 10^3$ at P60 were insufficient to prevent disease. Accordingly, we adoptively transferred AgX unfractionated T cells to P21 mice before the onset of disease and showed by histology at P30 that spontaneous development of EAU was arrested. Further experiments using FoxP3+CD25^{hi}CD4+ T_{reg} isolated from > P50 3A9 mice (naïve) or from > P50 dTg (AgX), showed that 3A9 T_{reg} were ineffective while AgX T_{reg}, not only halted disease progression but reversed the pathological changes (retinal vasculitis) in some cases. Further purified T_{reg} to deplete CD127+ cells were equally effective in preventing EAU development while Tx of CD25- T cells was ineffective. The T_{reg} enriched populations were negative for Eomes and were 97% Helios positive indicating that no Tr1 cells were included in the T_{reg} sample and that a significant proportion were (natural) nT_{reg} (52).

These data strongly suggest a dual mechanism of immunological tolerance in the retina, including regulation of autoreactive T cells both by T_{an} as well as by T_{reg}. They also point toward a therapeutic role for T_{reg} in immune-mediated diseases. There is considerable evidence for T_{reg} control of autoimmunity in many systems and their potential use in clinical autoimmune disease is under intensive investigation [reviewed in Esensten et al. (53)]. To generate sufficient numbers, T_{reg} may be expanded simply by administering IL2, an essential cytokine for T_{reg} growth (54), by accessory cell-based therapeutic regimes including tolerogenic DC [reviewed in Takenaka and Quintana (55)], or potentially by folate treatment (34). T_{reg}-specific upregulation of the folate surface receptor FR4 is commonly accepted, and likely expressed under the control of the FoxP3 transcription factor (34). It has been shown that T_{reg} require comparably large amounts of folate to stabilize their suppressive phenotype and retain high proliferative capacity *in vivo* (56). Conversely, CD4+ T cell populations, when depleted of nT_{reg} by functional blockade of the FR4 receptor, induce autoimmune disease after Tx to nude mice (34). Thus, signaling *via* the folate receptor appears to be critical for immune regulation and its role in reciprocal conversion of T_{reg} to T_{an} may be of

considerable relevance to the application of T_{reg} as a cell therapy for autoimmune disease. In the context of uveitis, T_{reg} are known to be involved in the control of experimental models (57) and appear to underpin the mechanisms of action of a number of standard clinical regimes (40). Control of uveitis by direct administration of T_{reg} has been shown for both systemic (16) and local application (58, 59).

Despite these promising reports, several questions require to be answered before T_{reg} cell therapy can become part of the therapeutic armamentarium. These include the effectiveness of antigen-specific vs. polyclonal T_{reg} (58), the “plasticity of T_{reg}” (60), the combined contribution of T_{an} and T_{reg} (this paper) and their site of action. In this study, the data support a local effect of T_{reg} as uveitis-suppressing T_{reg} appear to accumulate preferentially in the inflamed retina possibly *via* T_{an} (or *vice versa*), and previous work has shown the effectiveness of direct intravitreal inoculation of T_{reg} (59). On the other hand, the data in this study also suggest that AgX T cells are more effective than naive T cells, but it is possible that non-specifically activated T_{reg} may be equally effective. Hence, it remains to be clarified whether “spontaneous” uveitis as it occurs in this model of EAU is triggered by a quantitative imbalance in cell populations (e.g., [T_{reg}:T_{eff}]; [T_{reg}:T_{an}]) or if, qualitatively, “antigen-experienced” T_{reg} are essential and if so, whether tissue-specific antigen is necessary to control organ-specific disease. These experiments are in progress.

In conclusion, the model described in this report is reproducible, reliable and valuable for pre-clinical studies of therapies for uveitis and it opens up new avenues for research into mechanisms of tolerance in autoimmunity.

DATA AVAILABILITY STATEMENT

The datasets generated for this study are available on request to the corresponding author.

REFERENCES

- Kalekar LA, Mueller DL. Relationship between CD4 regulatory T Cells and anergy *In Vivo*. *J Immunol.* (2017) 198:2527–33. doi: 10.4049/jimmunol.1602031
- Fuchs A, Gliwinski M, Grageda N, Spiering R, Abbas AK, Appel S, et al. Minimum information about T regulatory cells: a step toward reproducibility and standardization. *Front Immunol.* (2017) 8:1844. doi: 10.3389/fimmu.2017.01844
- Lord P, Spiering R, Aguillon JC, Anderson AE, Appel S, Benitez-Ribas D, et al. Minimum information about tolerogenic antigen-presenting cells (MITAP): a first step towards reproducibility and standardisation of cellular therapies. *PeerJ* (2016) 4:e2300. doi: 10.7717/peerj.2300
- Romano M, Fanelli G, Albany CJ, Giganti G, Lombardi G. Past, present, and future of regulatory T cell therapy in transplantation and autoimmunity. *Front Immunol.* (2019) 10:43. doi: 10.3389/fimmu.2019.00043
- Caspi RR. A look at autoimmunity and inflammation in the eye. *J Clin Invest.* (2010) 120:3073–83. doi: 10.1172/JCI42440
- Forrester JV. Uveitis: pathogenesis. *Lancet.* (1991) 338:1498–501. doi: 10.1016/0140-6736(91)92309-p

ETHICS STATEMENT

The animal study was reviewed and approved by University of Aberdeen, Ethical Review Committee, University of Aberdeen, King's College, Aberdeen AB24 3FX, United Kingdom.

AUTHOR CONTRIBUTIONS

HW, LK, RC, and JF: study design. Y-HL, CM, KM, KK, CC, IK, DR, LK, and RC: *in vivo* and *in vitro* work/generation of data and materials. Y-HL, CM, KM, and KK: statistical analyses. Y-HL, CM, and JF: manuscript conceptualization and writing and formatting. All authors have critically revised the manuscript and agreed to its submission in the presented form.

FUNDING

This work was funded by Fight for Sight, The Eye Charity (CSO project grant award: 3031-3032), and The Development Trust of the University of Aberdeen (Saving Sight in Grampian) (Grant codes: RG-12663 and RG-14251).

ACKNOWLEDGMENTS

We thank the Iain Fraser Flow Cytometry core facility, and the Microscopy and Histology core facility of the University of Aberdeen.

SUPPLEMENTARY MATERIAL

The Supplementary Material for this article can be found online at: <https://www.frontiersin.org/articles/10.3389/fimmu.2020.02071/full#supplementary-material>

- Forrester JV, Kuffova L, Dick AD. Autoimmunity, autoinflammation and infection in uveitis. *Am J Ophthalmol.* (2018) 189:77–85. doi: 10.1016/j.ajo.2018.02.019
- Klaska IP, Forrester JV. Mouse models of autoimmune uveitis. *Curr Pharm Des.* (2015) 21:2453–67.
- Adamus G, Chan CC. Experimental autoimmune uveitides: multiple antigens, diverse diseases. *Int Rev Immunol.* (2002) 21:209–29.
- Gregerson DS, Torseth JW, McPherson SW, Roberts JP, Shinohara T, Zack DJ. Retinal expression of a neo-self antigen, beta-galactosidase, is not tolerogenic and creates a target for autoimmune uveoretinitis. *J Immunol.* (1999) 163:1073–80.
- Lambe T, Leung JC, Ferry H, Bouriez-Jones T, Makinen K, Crockford TL, et al. Limited peripheral T cell anergy predisposes to retinal autoimmunity. *J Immunol.* (2007) 178:4276–83.
- Liu YH, Corbett C, Klaska IP, Makinen K, Nickerson JM, Cornall RJ, et al. Partial retinal photoreceptor loss in a transgenic mouse model associated with reduced levels of interphotoreceptor retinol binding protein (IRBP. RBP3). *Exp Eye Res.* (2018) 172:54–65. doi: 10.1016/j.exer.2018.03.020
- Attridge K, Walker LS. Homeostasis and function of regulatory T cells (Tregs) *in vivo*: lessons from TCR-transgenic Tregs. *Immunol Rev.* (2014) 259:23–39. doi: 10.1111/imr.12165

14. Xu H, Koch P, Chen M, Lau A, Reid DM, Forrester JV. A clinical grading system for retinal inflammation in the chronic model of experimental autoimmune uveoretinitis using digital fundus images. *Exp Eye Res.* (2008) 87:319–26. doi: 10.1016/j.exer.2008.06.012
15. Barone F, Nayar S, Campos J, Cloake T, Withers DR, Toellner KM, et al. IL-22 regulates lymphoid chemokine production and assembly of tertiary lymphoid organs. *Proc Natl Acad Sci USA.* (2015) 112:11024–9. doi: 10.1073/pnas.1503315112
16. Siepmann K, Biester S, Plskova J, Muckersie E, Duncan L, Forrester JV. CD4+CD25+ T regulatory cells induced by LPS-activated bone marrow dendritic cells suppress experimental autoimmune uveoretinitis in vivo. *Graefes Arch Clin Exp Ophthalmol.* (2007) 245:221–9. doi: 10.1007/s00417-006-0356-9
17. Makinen K. *Spontaneous Model of Experimental Autoimmune Uveoretinitis: IRBP-HEL Transgenic Mice.* (2006). Ph.D. Thesis, University of Aberdeen, Aberdeen.
18. Liu W, Putnam AL, Xu-Yu Z, Szot GL, Lee MR, Zhu S, et al. CD127 expression inversely correlates with FoxP3 and suppressive function of human CD4+ T reg cells. *J Exp Med.* (2006) 203:1701–11. doi: 10.1084/jem.20060772
19. Tao R, de Zoeten EF, Ozkaynak E, Chen C, Wang L, Porrett PM, et al. Deacetylase inhibition promotes the generation and function of regulatory T cells. *Nat Med.* (2007) 13:1299–307. doi: 10.1038/nm1652
20. Van Parijs L, Peterson DA, Abbas AK. The Fas/Fas ligand pathway and Bcl-2 regulate T cell responses to model self and foreign antigens. *Immunity.* (1998) 8:265–74.
21. Akkaraju S, Ho WY, Leong D, Canaan K, Davis MM, Goodnow CC. A range of CD4 T cell tolerance: partial inactivation to organ-specific antigen allows nondestructive thyroiditis or insulinitis. *Immunity.* (1997) 7:255–71.
22. Hillhouse EE, Liston A, Collin R, Desautels E, Goodnow CC, Lesage S. TCR transgenic mice reveal the impact of type 1 diabetes loci on early and late disease checkpoints. *Immunol Cell Biol.* (2016) 94:709–13. doi: 10.1038/icb.2016.27
23. Forrester JV, Borthwick GM, McMenamin PG. Ultrastructural pathology of S-antigen uveoretinitis. *Invest Ophthalmol Vis Sci.* (1985) 26:1281–92.
24. Ager A. High endothelial venules and other blood vessels: critical regulators of lymphoid organ development and function. *Front Immunol.* (2017) 8:45. doi: 10.3389/fimmu.2017.00045
25. Funda DP, Golias J, Hudcovic T, Kozakova H, Spisek R, Palova-Jelinkova L. Antigen loading (e.g., glutamic acid decarboxylase 65) of tolerogenic DCs (tolDCs) reduces their capacity to prevent diabetes in the non-obese diabetes (n.d.)-severe combined immunodeficiency model of adoptive cotransfer of diabetes as well as in NOD mice. *Front Immunol.* (2018) 9:290. doi: 10.3389/fimmu.2018.00290
26. Horai R, Silver PB, Chen J, Agarwal RK, Chong WP, Jittayasothorn Y, et al. Breakdown of immune privilege and spontaneous autoimmunity in mice expressing a transgenic T cell receptor specific for a retinal autoantigen. *J Autoimmun.* (2013) 44:21–33. doi: 10.1016/j.jaut.2013.06.003
27. Luger D, Silver PB, Tang J, Cua D, Chen Z, Iwakura Y, et al. Either a Th17 or a Th1 effector response can drive autoimmunity: conditions of disease induction affect dominant effector category. *J Exp Med.* (2008) 205:799–810. doi: 10.1084/jem.20071258
28. Pipi E, Nayar S, Gardner DH, Colafrancesco S, Smith C, Barone F. Tertiary lymphoid structures: autoimmunity goes local. *Front Immunol.* (2018) 9:1952. doi: 10.3389/fimmu.2018.01952
29. Voigt V, Wikstrom ME, Kezic JM, Schuster IS, Fleming P, Makinen K, et al. Ocular antigen does not cause disease unless presented in the context of inflammation. *Sci Rep.* (2017) 7:14226. doi: 10.1038/s41598-017-14618-z
30. Liu YH, Mölzer C, Milne GC, Kuffova L, Forrester JV. Transmission electron microscopy data on drusen-like deposits in the retinal degeneration sTg-IRBP: HEL mouse model. *Data Brief.* (2019) 22:140–4. doi: 10.1016/j.dib.2018.12.007
31. Akkaraju S, Canaan K, Goodnow CC. Self-reactive B cells are not eliminated or inactivated by autoantigen expressed on thyroid epithelial cells. *J Exp Med.* (1997) 186:2005–12.
32. Morales MS, Mueller D. Anergy into T regulatory cells: an integration of metabolic cues and epigenetic changes at the Foxp3 conserved non-coding sequence 2 [version 1; peer review: 2 approved]. *F1000Research.* (2018) 7:1938. doi: 10.12688/f1000research.16551.1
33. Kalekar LA, Schmiel SE, Nandiwada SL, Lam WY, Barsness LO, Zhang N, et al. CD4(+) T cell anergy prevents autoimmunity and generates regulatory T cell precursors. *Nat Immunol.* (2016) 17:304–14. doi: 10.1038/ni.3331
34. Yamaguchi T, Hirota K, Nagahama K, Ohkawa K, Takahashi T, Nomura T, et al. Control of immune responses by antigen-specific regulatory T cells expressing the folate receptor. *Immunity.* (2007) 27:145–59. doi: 10.1016/j.immuni.2007.04.017
35. Peterson DA, DiPaolo RJ, Kanagawa O, Unanue ER. Cutting edge: negative selection of immature thymocytes by a few peptide-MHC complexes: differential sensitivity of immature and mature T cells. *J Immunol.* (1999) 162:3117–20.
36. Liou GI, Fei Y, Peachey NS, Matragoon S, Wei S, Blaner WS, et al. Early onset photoreceptor abnormalities induced by targeted disruption of the interphotoreceptor retinoid-binding protein gene. *J Neurosci.* (1998) 18:4511–20.
37. Tan LT, Isa H, Lightman S, Taylor SR. Prevalence and causes of phthisis bulbi in a uveitis clinic. *Acta Ophthalmol.* (2012) 90:e417–8. doi: 10.1111/j.1755-3768.2011.02319.x
38. Unanue ER, Ferris ST, Carrero JA. The role of islet antigen presenting cells and the presentation of insulin in the initiation of autoimmune diabetes in the NOD mouse. *Immunol Rev.* (2016) 272:183–201. doi: 10.1111/imr.12430
39. Von Boehmer H. Deciphering thymic development. *Front Immunol.* (2014) 5:424. doi: 10.3389/fimmu.2014.00424
40. Lee RW, Nicholson LB, Sen HN, Chan CC, Wei L, Nussenblatt RB, et al. Autoimmune and autoinflammatory mechanisms in uveitis. *Semin Immunopathol.* (2014) 36:581–94. doi: 10.1007/s00281-014-0433-9
41. Huppa JB, Davis MM. The interdisciplinary science of T-cell recognition. *Adv Immunol.* (2013) 119:1–50. doi: 10.1016/B978-0-12-407707-2.00001-1
42. Kreslavsky T, Von Boehmer H. Gammadelta TCR ligands and lineage commitment. *Semin Immunol.* (2010) 22:214–21. doi: 10.1016/j.smim.2010.04.001
43. Kreslavsky T, Gleimer M, von Boehmer H. Alphabeta versus gammadelta lineage choice at the first TCR-controlled checkpoint. *Curr Opin Immunol.* (2010) 22:185–92. doi: 10.1016/j.coi.2009.12.006
44. Hillhouse EE, Lesage S. A comprehensive review of the phenotype and function of antigen-specific immunoregulatory double negative T cells. *J Autoimmun.* (2013) 40:58–65. doi: 10.1016/j.jaut.2012.07.010
45. Voehringer D, Liang HE, Locksley RM. Homeostasis and effector function of lymphopenia-induced “memory-like” T cells in constitutively T cell-depleted mice. *J Immunol.* (2008) 180:4742–53.
46. Kielczewski JL, Horai R, Jittayasothorn Y, Chan CC, Caspi RR. Tertiary Lymphoid tissue forms in retinas of mice with spontaneous autoimmune uveitis and has consequences on visual function. *J Immunol.* (2016) 196:1013–25. doi: 10.4049/jimmunol.1501570
47. Takatori H, Kanno Y, Watford WT, Tato CM, Weiss G, Ivanov II, et al. Lymphoid tissue inducer-like cells are an innate source of IL-17 and IL-22. *J Exp Med.* (2009) 206:35–41. doi: 10.1084/jem.20072713
48. Grogan JL, Ouyang W. A role for Th17 cells in the regulation of tertiary lymphoid follicles. *Eur J Immunol.* (2012) 42:2255–62. doi: 10.1002/eji.201242656
49. Mattapallil MJ, Kielczewski JL, Zarate-Blades CR, St Leger AJ, Raychaudhuri K, Silver PB, et al. Interleukin 22 ameliorates neuropathology and protects from central nervous system autoimmunity. *J Autoimmun.* (2019) 102:65–76. doi: 10.1016/j.jaut.2019.04.017
50. McPherson SW, Heuss ND, Gregerson DS. Lymphopenia-induced proliferation is a potent activator for CD4+ T cell-mediated autoimmune disease in the retina. *J Immunol.* (2009) 182:969–79.
51. McPherson SW, Heuss ND, Pierson MJ, Gregerson DS. Retinal antigen-specific regulatory T cells protect against spontaneous and induced autoimmunity and require local dendritic cells. *J Neuroinflammation.* (2014) 11:205. doi: 10.1186/s12974-014-0205-4
52. Zhu J, Paul WE. Peripheral CD4+ T-cell differentiation regulated by networks of cytokines and transcription factors. *Immunol Rev.* (2010) 238:247–62. doi: 10.1111/j.1600-065X.2010.00951.x
53. Esensten JH, Muller YD, Bluestone JA, Tang Q. Regulatory T cell therapy for autoimmune and autoinflammatory diseases: the next frontier. *J Allergy Clin Immunol.* (2018) 142:1710–8. doi: 10.1016/j.jaci.2018.10.015

54. Klatzmann D, Abbas AK. The promise of low-dose interleukin-2 therapy for autoimmune and inflammatory diseases. *Nat Rev Immunol.* (2015) 15:283–94. doi: 10.1038/nri3823
55. Takenaka MC, Quintana FJ. Tolerogenic dendritic cells. *Semin Immunopathol.* (2017) 39:113–20. doi: 10.1007/s00281-016-0587-8
56. Sakaguchi S, Yamaguchi T, Nomura T, Ono M. Regulatory T cells and immune tolerance. *Cell.* (2008) 133:775–87. doi: 10.1016/j.cell.2008.05.009
57. Lau AW, Biester S, Cornall RJ, Forrester JV. Lipopolysaccharide-activated IL-10-secreting dendritic cells suppress experimental autoimmune uveoretinitis by MHCII-dependent activation of CD62L-expressing regulatory T cells. *J Immunol.* (2008) 180:3889–99.
58. Foussat A, Gregoire S, Clerget-Chossat N, Terrada C, Asnagli H, Lemoine FM, et al. Regulatory T cell therapy for uveitis: a new promising challenge. *J Ocul Pharmacol Ther.* (2017) 33:278–84. doi: 10.1089/jop.2016.0165
59. Gregoire S, Terrada C, Martin GH, Fourcade G, Baeyens A, Marodon G, et al. Treatment of uveitis by in situ administration of ex vivo-activated polyclonal regulatory T cells. *J Immunol.* (2016) 196:2109–18. doi: 10.4049/jimmunol.1501723
60. Hori S. Lineage stability and phenotypic plasticity of Foxp3(+) regulatory T cells. *Immunol Rev.* (2014) 259:159–72. doi: 10.1111/imr.12175

Conflict of Interest: The authors declare that the research was conducted in the absence of any commercial or financial relationships that could be construed as a potential conflict of interest.

Citation: Liu Y-H, Mölzer C, Makinen K, Kamoi K, Corbett CLC, Klaska IP, Reid DM, Wilson HM, Kuffová L, Cornall RJ and Forrester JV (2020) Treatment With FoxP3+ Antigen-Experienced T Regulatory Cells Arrests Progressive Retinal Damage in a Spontaneous Model of Uveitis. *Front. Immunol.* 11:2071. doi: 10.3389/fimmu.2020.02071

Copyright © 2020 Liu, Mölzer, Makinen, Kamoi, Corbett, Klaska, Reid, Wilson, Kuffová, Cornall and Forrester. This is an open-access article distributed under the terms of the Creative Commons Attribution License (CC BY). The use, distribution or reproduction in other forums is permitted, provided the original author(s) and the copyright owner(s) are credited and that the original publication in this journal is cited, in accordance with accepted academic practice. No use, distribution or reproduction is permitted which does not comply with these terms.